LA-UR-97-1520

C.34

Title: **High-Energy Test of Proton Radiography Concepts**

Author(s): **J. F. Amann, C. J. Espinoza, J. J. Gomez, G. W. Hart, G. E. Hogan, L. J. Marek, J. B. McClelland, C. L. Morris, H. J. Ziock, and J. D. Zumbro, P-25; L. G. Atencio, P-21; R. E. Hill, S. A. Jaramillo, N. S. P. King, K. B. Morley, P. Pazuchanics, and G. J. Yates, P-23; C. T. Mottershead, LANSCE-1; K. H. Mueller, DX-3; and J. S. Sarracino, X-NH; A. Saunders, Univ. Colorado; E. P. Hartouni, LLNL; R. Prigl, J. Scaduto and E. Schwaner, BNL**

Submitted to: **DOE Office of Scientific and Technical Information (OSTI)**

Los Alamos
NATIONAL LABORATORY

High-Energy Test of Proton Radiography Concepts

J. F. Amann, L. G. Atencio, C. J. Espinoza, J. J. Gomez, G. W. Hart, R. E. Hill, G. E. Hogan, S. A. Jaramillo, N. S. P. King, L. J. Marek, J. B. McClelland, K. B. Morley, C. L. Morris*, C. T. Mottershead, K. H. Mueller, P. Pazuchanics, J. S. Sarracino, G. J. Yates, H. J. Ziock, and J. D. Zumbro
Los Alamos National Laboratory

A. Saunders
University of Colorado

E. P. Hartouni
Lawrence Livermore National Laboratory

R. Prigl, J. Scaduto and E. Schwaner
Brookhaven National Laboratory

Abstract

This is the final report of a one-year, Laboratory-Directed Research and Development (LDRD) project at the Los Alamos National Laboratory (LANL). The goal of this work was to demonstrate the use of high energy protons to produce radiographs of heavy metal test objects. We executed a proof-of principle experiment using GeV proton beams available at the Brookhaven National Laboratory Alternating Gradient Synchrotron (AGS). The experiment produced proton radiographs of a suitably dense, unclassified test object. The experiment tested capabilities in data collection, image reconstruction, and hydro-code simulation and validated models of high-energy proton radiography. A lens was designed using existing quadrupole magnets, constructed on the A1 beam line of the AGS and used to image 10-GeV protons. The results include: 1) images made with an integrating detector, 2) measurements of the background and measurements of the resolution functions, and 3) forward model fits to the transmission data. In all cases the results agree with initial estimates and provide strong support for the utility of proton radiography as a new hydrotest diagnostic.

1. Background and Research Objectives

Los Alamos National Laboratory has had a dominant role for many years in hydrodynamic radiography using its PHERMEX RF electron-beam linear accelerator as a source for X-radiography. In May 1994, LANL began construction of its Dual Axis Radiographic Hydrodynamic Test (DARHT) facility to advance the state of X-ray radiography

*Principal Investigator, e-mail: cmorris@lanl.gov

by achieving flash radiographs on two axis simultaneously. Recently, a promising new approach has emerged from research conducted at LANL, using protons as the radiographic probe.[1] This approach appears to have several important advantages over traditional X-ray radiography and has promise as a diagnostic of weapons primary hydrodynamic tests and as a way to further advance the field of radiography.

Thus far, several proton experiments have been performed on static objects with great success. Simulations and some experimental effort have moved proton radiography from being an unexplored technology to being one that appears to be able to meet all of the goals for advanced radiography. Some of the advantages of protons over conventional X-ray techniques for radiographing thick, dense, dynamic systems include (1) high penetrating power, (2) high detection efficiency, (3) very small scattered background, (4) no need for a conversion target and the consequent phase space broadening of the beam, (5) inherent multipulse capability, and (6) the ability to tolerate large standoff distances from the test object and containment vessel for both the incoming and outgoing beam. These capabilities reflect the fact that protons interact with matter through both the long-range Coulomb force and the short-range strong interaction. The ability to focus protons using a magnetic lens allows the magnitude and Z-dependence of the interaction to be changed simply by looking at an object through different angular apertures. This leads to a material composition assessment capability. Multiple images can be made on a single axis by using multiple detectors, lenses, and irises.

This report describes the setup and running of experiments at the Alternating Gradient Accelerator (AGS) at Brookhaven National Laboratory to demonstrate proton radiography with a high energy proton beam. The first experiment was performed in April on the B2 test beam and used tracking chambers to simulate a perfect lens. The second experiment involved the design, set up and testing of a beam line, quadrupole lens system, and detectors on the A1 beam line. The goals were to demonstrate images of test objects, measure the background and position resolution of the images, and to perform quantitative analysis to demonstrate the expected precision of mass density measurements and material sensitivity of proton radiography.

2. Importance to LANL's Science and Technology Base and National R&D Needs

The decision to cease underground nuclear testing and the commitment to reduce the nuclear stockpile to an increasingly smaller number of weapons has forced the Department of Energy (DOE) and its laboratories to rethink their role in stockpile stewardship. Much of this reassessment has been embodied in the philosophy of science-based rather than test-based

stockpile stewardship. This policy has required the DOE and its three nuclear weapons research and development laboratories to rely on other, zero yield methods to assess the safety, reliability, and performance of the nuclear weapons stockpile.

One of the most important of these methods will be above-ground dynamic experiments aimed at constraining the physical parameters needed to model weapon primary performance. Proton radiography will provide new diagnostics for dynamic testing. Recent developments and simulations suggest that proton radiography can provide density measurements at previously unobtainable precision and in previously inaccessible thickness regimes. This project was aimed at validating simulations and showing that the suggested techniques can be implemented in a practical experiment.

3. Scientific Approach and Accomplishments

Proton radiography has much in common with X-ray radiography in that the areal densities of the object under study are determined by measuring the attenuation of the beam incident on an object under study. However, a fundamental difference arises due to the Coulomb interaction between the incident beam and the object being radiographed. All transmitted protons interact in the material of the object. Protons have their angles changed due to Coulomb scattering from the heavy atomic nuclei in the material and their energies changed due to Coulomb scattering from the light electrons in the material.

Position Resolution

Position broadening due to multiple scattering can be mitigated by using a lens to image the protons transmitted by an object onto a detector. It is this innovation which has made proton radiography possible for thick objects. With a lens system the position resolution and mass density uncertainty that can be obtained in proton radiography of a single component system of length l can be understood from some basic considerations. The position uncertainty that can be obtained at the center of the object has two contributions. The first results from the deviation of the particle from a straight line due to multiple scattering in the material and is given to first order by[2]:

$$\Delta x_{ms} = \frac{\theta_0 l}{2\sqrt{6}}$$

where l is the length through an object and θ_0 is the multiple scattering angle:

$$\theta_0 = \frac{14.1}{p\beta}\sqrt{\frac{l}{L_R}}$$

assuming that the entire angular cone given by multiple scattering is accepted. Here, p is the beam momentum, and β is the beam velocity measured in units of the speed of light. The quantity L_R is the length over which a high energy electron loses on average all but 1/e of its energy to Bremsstrahlung and is a property of material that varies approximately as Z^2/A where Z is the atomic charge and A is the atomic number of the medium.

Another contribution arises from the aberrations in the lens system. By using a matching lens many of the aberrations in the lens system can be reduced to small levels, leaving the lowest-order chromatic term dominant. Simulations have shown that this contribution to the position resolution is given approximately by:

$$\Delta x = < x|\theta\delta > \theta\delta$$

Here Δx is the position resolution, θ is the angular acceptance of the lens, and δ is the fractional-momentum spread in the beam to be focused. Actual designs at 10 GeV yield a lens with a value of about 20 m for the term $<x|\theta\delta>$, which is the leading chromatic term in simple quadrupole lens systems. For most of the quadrupole lenses we have studied, the $<x|\theta\delta>$ term is a little bit larger than the length of the lens systems.

The physical processes of Coulomb scattering from the electrons and atomic nuclei in the medium to be radiographed determine intrinsic values for θ and δ for a given system. Multiple-Coulomb scattering was discussed above. In order to obtain the best signal to noise and the lowest statistical uncertainty in transmission radiography, it is desirable to match the acceptance of the lens to the multiple-scattering cone. The energy loss through a material with thickness, l, is given by:

$$\Delta T = \int_0^l \frac{dE}{dx} dl \approx \frac{dE}{dx} l.$$

The quantity dE/dx is approximately independent of kinetic energy at energies above $\approx 1/2$ of the incident particle mass, M. The fractional-momentum spread due to the energy loss is given by:

$$\delta = \frac{T+M}{T+2M}\frac{\Delta T}{T}$$
$$= 0.92\frac{\Delta T}{T} \text{ at 10 GeV.}$$

At high energies where ΔT is approximately constant, δ is inversely proportional to the energy.

The factors that determine the spatial resolution are inversely proportional to momentum in the case of multiple scattering in the object or momentum squared in the case of chromatic lens aberrations (i.e. higher momentum yields smaller Δx). At 10 GeV the fractional-momentum loss through a typical test object is about 3% and the multiple scattering angle is about θ_0=10 mr. Thus one expects a contribution of the lens to the resolution of about 6 mm σ over the entire thickness range spanned by the object. Protons of near 10 GeV are available as secondary beams at the AGS

Mass density resolution

Conventional radiography uses the attenuation of the flux transmitted through an object to determine it's thickness, l, in units of areal density on an array of pixels. The transmitted intensity for a pixel, N, is related to the incident beam intensity, N_0 by:

$N = N_0 e^{-\Sigma \frac{l_i}{\lambda_i}}$, $\lambda_i = \frac{1}{\rho_i \sigma_i}$, where ρ is the density, and σ is the cross section.

For a single component system:

$$l = \lambda \ln\left(\frac{N}{N_0}\right).$$

The error in l is given by:

$\Delta l = \frac{dl}{dN}\Delta N$, which gives

$$\Delta l = \frac{\Delta N}{N}\lambda = \sqrt{\frac{1}{N}}\lambda.$$

These results assume a perfect detector and no uncertainty in the incident flux. Obtaining a precision of 1% for an object one mean free path thick requires an integrated transmitted particle flux of 10^4 particles. By further manipulation we can show that there is an ideal mean free path (an ideal probe) for radiographing a system with a given thickness:

$$\frac{\partial(\Delta l)}{\partial\lambda}=0\Rightarrow\frac{\partial}{\partial\lambda}\left(\lambda\frac{e^{-\frac{l}{2\lambda}}}{N_0}\right)=0$$

$$e^{-\frac{l}{2\lambda}}-\frac{l}{2\lambda}e^{-\frac{l}{2\lambda}}=0\Rightarrow\lambda=\frac{l}{2}$$

High energy proton beams, with a mean free path of about 200 gm/cm^2 in uranium, are ideally matched to the systems used in hydrotest modeling of weapons primaries.

Another radiographic measurement can be made using the attenuation due to multiple scattering outside of an aperture. The angular distribution due to multiple scattering is given by:

$$\frac{dN}{d\theta}=\frac{1}{2\pi\theta_0^2}e^{\frac{\theta^2}{2\theta_0^2}},$$

This can be integrated from 0 to some aperture, θ_c, to give:

$$N_2=N_1(1-e^{\frac{\theta_c^2}{2\theta_0^2}}),$$

An expression for the length through a single component (for simplicity) can be obtained as:

$$l=-\frac{k}{\ln(1-\frac{N_2}{N_1})}\text{ where }k=\frac{(p\beta\theta_c)^2}{2(14.1)^2}L_R,\text{ and the fractional error in }l\text{ is given by:}$$

$$\frac{\Delta l}{l}=-\frac{1}{\ln(1-R)}\sqrt{\frac{R}{(1-R)}}\frac{\Delta N_1}{N_1}\text{ where }R=\frac{N_2}{N_1}.$$

N_1 is the flux transmitted through the object, N_2 is the flux transmitted through an angular aperture, θ_c. Data from two different angular apertures can be analyzed to provide both thickness and composition information because of the differential behavior of λ and θ_0 for different materials. This possibility provides proton radiography with the unique capability of identifying the material composition when used in flash radiography.

Test Beam Run

Experiments performed at the Los Alamos Neutron Science Center (LANSCE) in FY95 using beams of 188- and 300-MeV protons have demonstrated many of the concepts of proton radiography as applied to thin systems. However, at low momentum, position-blurring due to multiple scattering limits the resolution obtainable for thick objects. The resolution is potentially further limited by energy loss variation across the object when a magnetic imaging system is used. While scaling the LANSCE results to higher energies is conceptually possible, it is clear that additional physics comes into play in the proton transport and must be benchmarked by experiments.

This project supported a March run at the AGS where we demonstrated the contrast and quantitative nature of the data that can be obtained in an experiment using tracking chambers (the equivalent of a perfect lens) with an 8-GeV/c proton beam on the French Test Object (FTO), shown in figure 1, at the AGS test beam line (B2). Figure 2 shows an online radiograph of the FTO obtained in a one-hour period. Even though further calibration including compensation for the spatial non-uniformity of the beam and better statistics will improve the image quality, details of the object are clearly visible. These data were taken with a new PC-based data acquisition system developed specifically for this run.

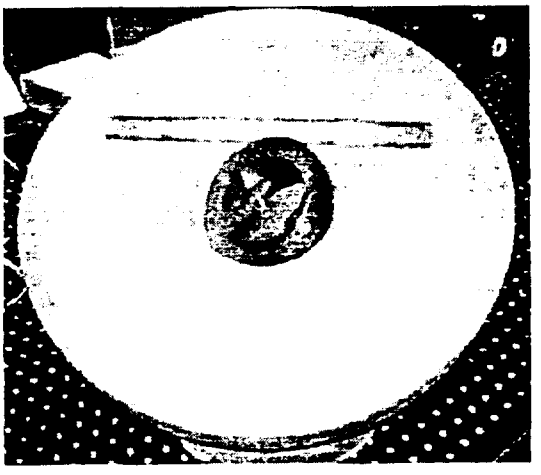

Figure 1. The French Test Object consists of a concentric set of spherical shells made from the half shells shown above. The inner shell is made of tungsten with a central cavity, followed by copper and then foam. The maximum thickness of the object as seen by the proton beam is approximately 180 g/cm^2.

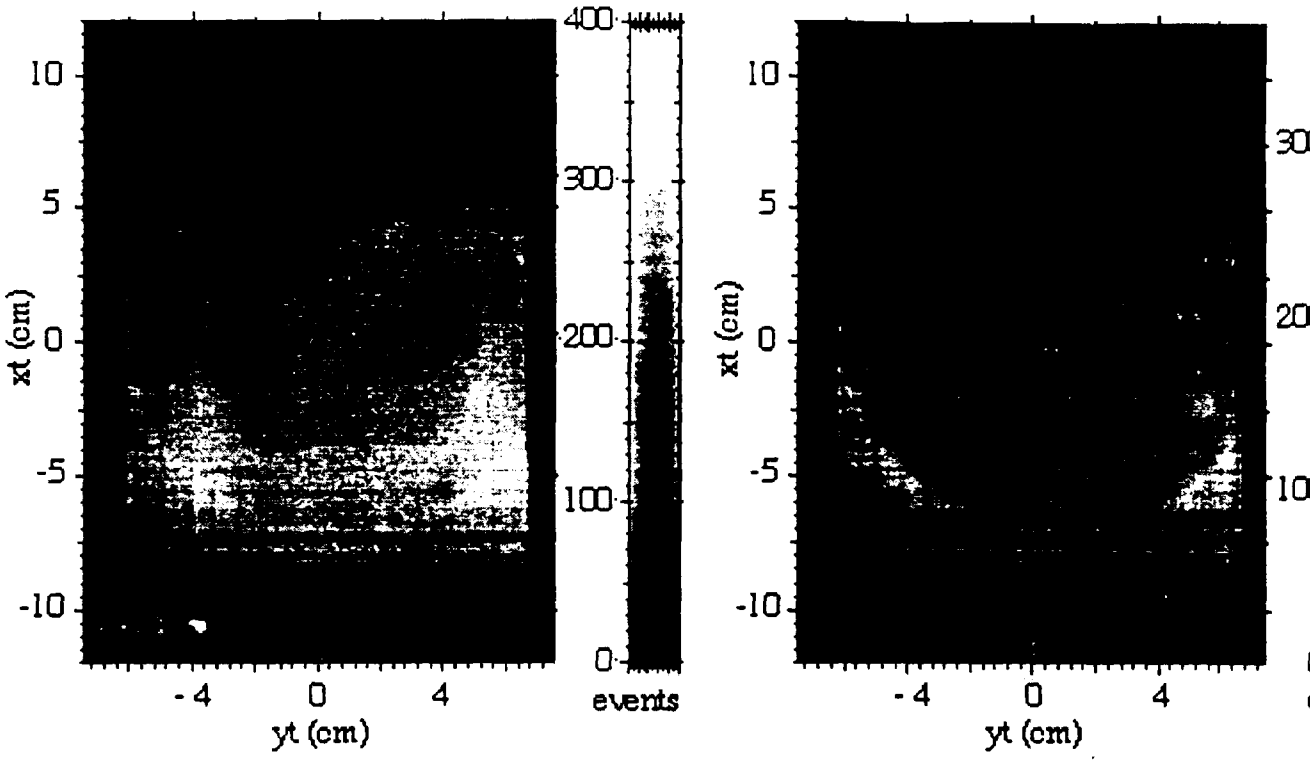

Figure 2. Online radiographs of the FTO obtained with an 8 GeV/c beam on the B2 test beam line at the AGS. The radiographs predominately show the inner 3 shells, consisting of copper, tungsten, and air. The images were obtained in one hour of running with a total of about 4×10^7 incident protons. The gray scale indicates the number of particles per 1-mm^2 bin. The left frame was obtained using a 20-milliradian angular cut with respect to the beam axis while the right frame used a 7-milliradian cut. As expected, the apparent contrast between the tungsten and copper shells is enhanced when the more highly deflected protons are rejected.

Data Acquisition System

The experiments performed at the AGS required the ability to take event mode data. No suitable software existed for this task, either because of licensing problems or because of antiquated hardware. In developing a new DAQ system, we had several objectives in mind.

Replacement for the Q/VAX system. The Q data acquisition system developed at LAMPF/LANSCE is no longer supported in either its software or hardware components. We needed a new DAQ system that is supportable.

Software Licensing. Many DAQ/Analysis systems use the CERN library as a source of programs for analysis and plotting. However, because of the nature of the Proton Radiography project, use of the CERN library is not appropriate. We also wanted to avoid expensive, single-purpose licenses such as LABVIEW® as it is anticipated that our computer program will be used on many platforms.

Computer Hardware. We wanted a computer hardware platform that is powerful and inexpensive.

DAQ Hardware. Moderate amounts of CAMAC hardware have been inherited from the shutdown of LAMPF. A CAMAC-based DAQ system could reuse this capital investment.

Programmer Expertise. Because of the considerable time pressure to develop a new system, adopting a familiar programming environment would speed up the development process. A system modeled on the LAMPF Q system would make it easier for users at LANL to learn a new system.

Our new system, named PC DAQ, meets these objectives. As a DAQ system, its general design is based on the Q system. It handles multiple types of triggers and uses the same syntax to define histograms and histogram tests. The code is developed in-house. The only licenses needed are for languages; Visual Basic 4.0, FORTRAN PS 4.0, and Visual C++ 4.0 or above. The newer Pentium and Pentium Pro chips meet the computer hardware needs. Finally, the principal author (Gary Hogan) already has experience writing Windows/Visual Basic DAQ systems.

PC DAQ is designed to run on a 32-bit Windows® operating system (Windows 95®, Windows NT 3.51®, or above) running on the INTEL® 80x86 processor line. It is written in a combination of Microsoft Visual Basic 4.0 (VB), Visual C++ 4.0, and FORTRAN Power Station 4.0. The user interface is written in VB. The analysis routines are in FORTRAN. All user supplied routines are in FORTRAN. A small amount of code exists in C++.

For 16-bit words, transfer speeds of up to 400 Kbytes/sec in DMA mode have been achieved. The program provides both DAQ and replay (disk file input) modes. Histograming, testing, and plotting packages are provided. Histogram data can be exported to spreadsheets or analyzed in user supplied programs. A run-keyed database is provided.

A number of other experiments outside of Proton Radiography are looking into the possibility of using our computer program. They include neutron experiments at LANSCE and nuclear physics experiments at the Brookhaven AGS.

Lens demonstration

A suitable lensing system is crucial to the success of proton radiography due to the blurring effects of multiple Coulomb scattering. An elegant solution capable of sub-millimeter resolution at high enough energies using existing magnets has been developed, the Zumbro identity lens (ZI). The AGS was ideally suited to test this design, which was built from

existing magnets and used a secondary proton beam on the A1 line in a run in June/July 1996. The lens tests used the detectors and data acquisition system set up for the March run on the B2 test beam line. The choice of a beam energy of 10 GeV was dictated by the maximum field strengths of the existing magnets and the physical space available.

The ZI solution provides X-Y symmetric, inverted point-to-point imaging in space, as well as negative unit mapping of angles from the source. The high degree of symmetry in this solution minimizes aberrations. A complete radiographic focusing system would consist of two subsystems of this type, with the second, downstream subsystem containing a smaller defining aperture to provide the capability for a second, multiple scattering radiograph of the test object. Two images obtained on a single axis can be used to obtain information on material composition and amount, which greatly simplifies the interpretation of a dynamic radiograph. In the current experiment we tested this concept by making multiple images through a single lens using two different apertures.

The second order matrix element $\langle x|\theta\delta\rangle$ for this system is about 21 m and is the dominant source of aberrations for this lens system. For the FTO, the range of δ in the central region is about 0.5% for an incident beam energy of 10 GeV and about 3% over the entire object. The multiple scattering angle is less than 10 mrad. Combining these numbers we find that the maximum size of this aberration over the central region of the object was expected to be about 1 mm. This is comparable to the best point spread functions proposed for the next generation of pulsed X-ray machines.

The complete system used 5-8Q48 and 2-12Q24 quadrupole magnets; the first three quadrupoles form the condenser and produce the desired beam spot at the object, and the last four quadrupoles form the imaging lens. The system is shown in Figure 3.

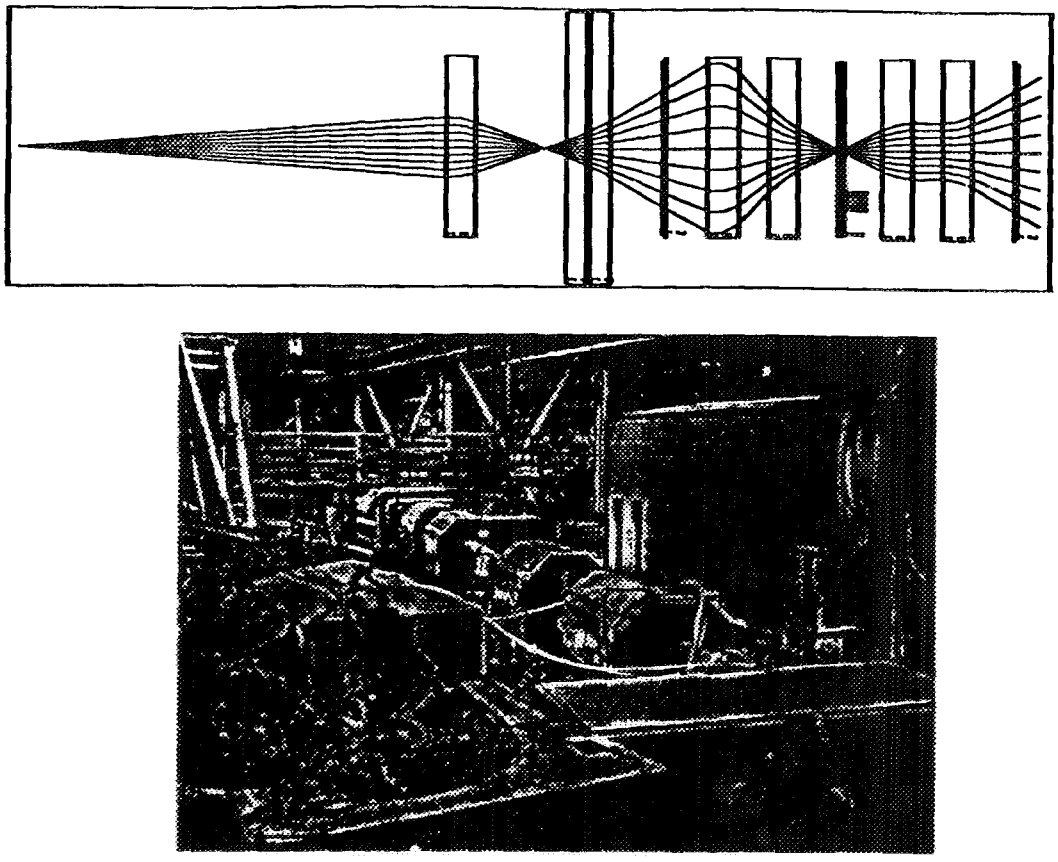

Figure 3. Top: Beam envelope calculations through the lens system. Bottom: Photograph showing the quadrapole magnets in place at the AGS.

Image Plate FTO Image

One question left over from the test beam run was whether or not there was a background of low momentum particles, due to diffractive dissociation, which would be imaged by the tracking system but not by a magnetic lens because of chromatic aberrations. This was answered shortly after we obtained our first proton beam by making an image with an image plate detector in the focal plane of the magnet lens. The image plates are like film in that they respond to all incident particles in an unbiased way but are unlike film in that the response is linear over a wide dynamic range. An image of the FTO obtained using these image plates is shown as Figure 4.

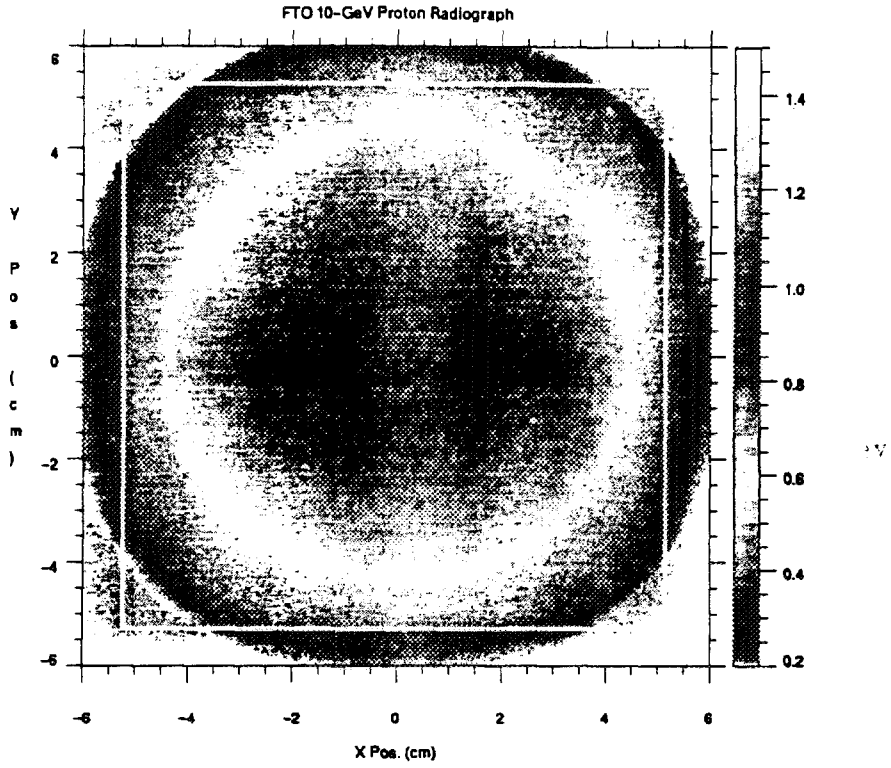

Figure 4. Image of the FTO made by computing the ratio of an image with the FTO in the beam to an image with the FTO removed. The white border shows the calculated clear field of view of the lens system.

The root mean square of fractional fluctuations from a smooth curve in a line scan across an image plate image were used to estimate the detector quantum efficiency (DQE) of an image plate for protons. The DQE allows one to estimate the particle exposure, N, necessary to achieve a given statistical precision, P, as

$$N = \frac{1}{P^2 \times DQE}$$

We inverted the preceding equation to solve for the DQE of the image plates as we knew N for the exposure and determined P from analyzing scans. The result was 20%. Large fluctuations on a few pixels dominated this result. We found that by stacking image plates, we could significantly increase the DQE. This was because the infrequent large fluctuations were not

correlated from plate to plate. The image shown in Figure 4 is the average of five simultaneously exposed plates.

Background Measurement

The data acquisition system and tracking chambers located both upstream and downstream of the object allowed us to measure the resolution function of the imaging system and to identify and quantify background in the image plane. The trajectory information from the upstream chambers was used to calculate the position of an incident particle at the center of the object. The sum of this position and the position of the same particle in the focal plane of the lens, calculated using the information from the downstream chambers, could be used to measure the resolution function of the lens system, due to the fact that we had an inverting identity lens, $x_{image} = -x_{object}$ and $y_{image} = -y_{object}$. Histograms of these position sums, in both the horizontal (XSUM) and vertical (YSUM) directions, are displayed in Figure 5.

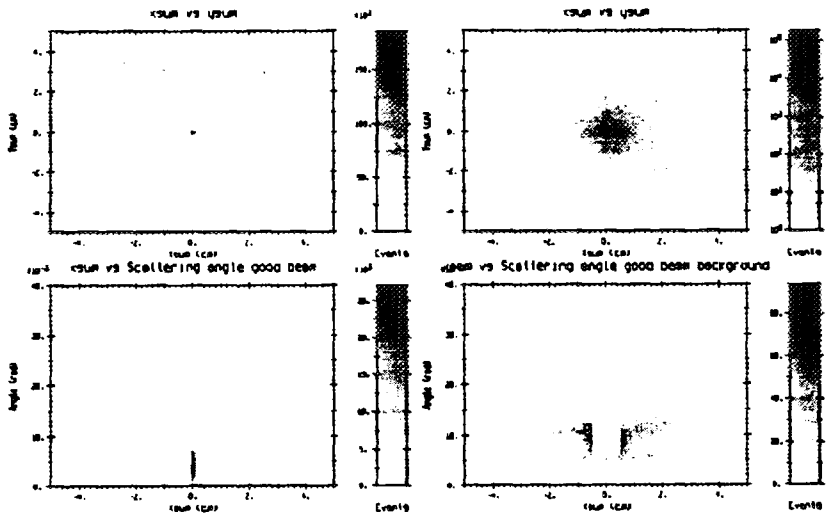

Figure 5. Top left: two-dimensional histogram of the X vs. Y position sum on a linear scale. Top right: on a logarithmic scale. Bottom left: X position sum vs. scattering angle on a linear scale. Bottom right: on a logarithmic scale with the additional condition that both the XSUM and YSUM be larger than 5 mm.

Background events could be identified as those whose XSUM and YSUM where outside of reasonable limits. An example is shown on the bottom histograms in Figure 5, where the scattering angle in the object, calculated by comparing the upstream and downstream trajectory information, is plotted versus XSUM. A band of events at large scattering angle is seen to dominate the background in these plots.

This technique was used to identify three sources of background. 1) Events that were outside of the clear acceptance of the lens and that scattered from the vacuum pipe or magnet pole faces and were detected in the focal plane (large near the edge of the acceptance); 2) Events that scattered from the collimator, the horizontal band observed in Figure 5 (5% at the center of the object); and 3) The remaining background which was assumed to be dominated by secondary particles or by protons which had their energy degraded by processes such as diffractive dissociation (2% at the center of the object). Histograms comparing these backgrounds with the transmitted data are shown in Figure 6.

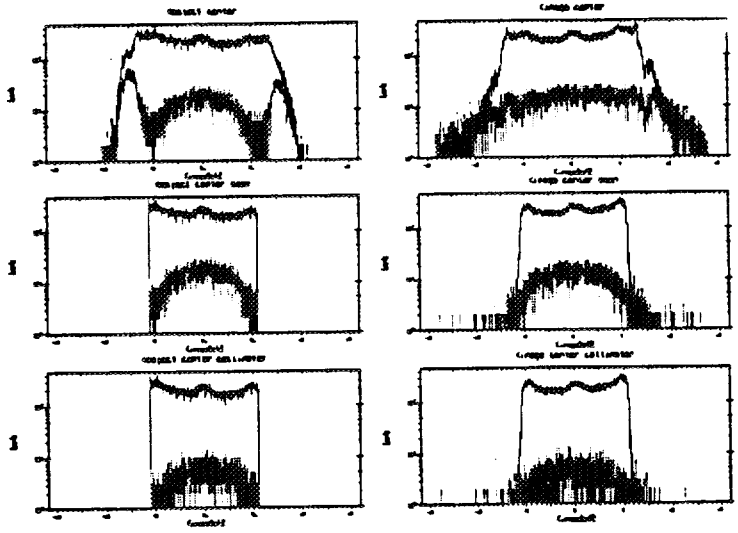

Figure 6. Left: histograms of X positions at the object plane for events within a 1 cm wide band in Y centered on the object. Right: histograms of positions at the image plane. Top: all events. Middle: events required to be in the lens field of view at the object. Bottom: events required to within the collimator acceptance. The top lines are the signal plus background and the bottom lines are the background.

The background from the first two sources can be reduced by more careful design of the collimation of the incident beam and of the scattering angle collimator in the lens. Measurements made subsequent to the experiment have shown the magnetic fields in this collimator were much lower than designed.

Data Fitting

The data obtained with the wire chambers were fitted to reconstruct the object and estimate the quality of quantitative reconstruction using proton radiography. More work remains to be done in this effort but some typical results are shown in Figure 7. The data fitted

were restricted to events surviving cuts that removed the backgrounds due to particles outside of the field of view of the lens and scattering in the collimator.

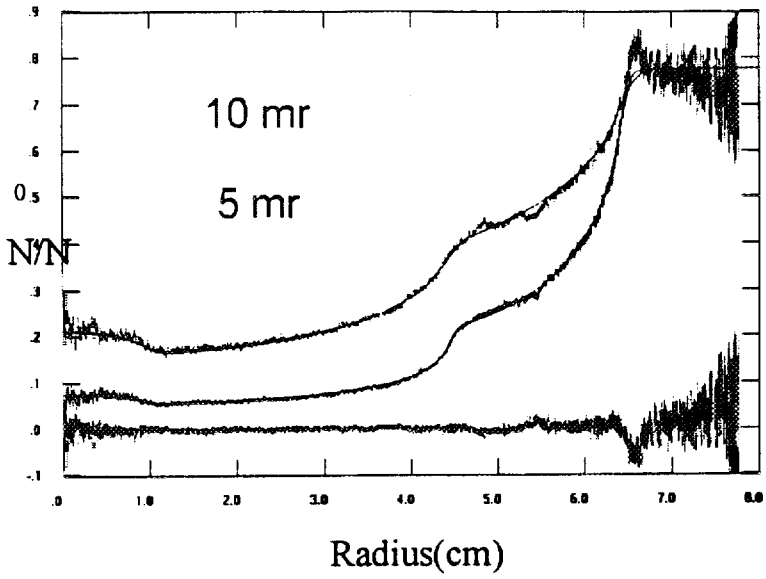

Figure 7. Fits to the transmission data through the FTO. The two upper wiggly curves are the measured transmission versus radius (10 mr and 5 mr, respectively). The fine lines through these data are the fitted transmissions. Bottom data points are the residuals of the fit.

The transmission was calculated by taking the ratio of the transmitted beam (measured in the downstream chambers) to the beam profile (measured by the data in the upstream chambers). An initial fit to a two-dimensional histogram of the transmission was performed to establish the center of the object. A Gaussian blurring function was applied to the beam profile to approximate the effects of multiple scattering and lens aberrations. The fitted size of the blurring was 1.2 mm. The modeled object consisted of the concentric spherical shells. The radii, attenuation lengths and radiation lengths for the two inner shells were varied.

The fitted radii, attenuation lengths, and radiation lengths for the tungsten region of the FTO agree fairly well with expectations. In a series of fits, the three boundary radii are fitted to better than 100 μm. The fitted density of the tungsten agrees with its actual value to better than 3%, using handbook values for the attenuation lengths. This is approaching the level of quantitative agreement necessary to meet the AHF requirements for criticality measurements. The density of the copper is reproduced to better than 10%. We expect that when the results of measurements made with a step wedge are included, the agreement will improve.

Conclusions

This LDRD project supported work at the AGS aimed at validating models of high energy proton radiography. A lens was designed using existing quadrupole magnets, constructed on the A1 beam line of the AGS, and used to image 10 GeV protons. The results include: 1) images made with an integrating detector, 2) measurements of the background and the resolution functions, and 3) forward model fits to the transmission data. In all cases the results agree with initial estimates and provide strong support for the utility of proton radiography as a new hydrotest diagnostic.

References

[1] A. Gavron, C. L. Morris, H. J. Ziock, and J. D. Zumbro, "Proton radiography," LA-UR-96-420, (1996).

[2] B. Rossi, "High-Energy Physics," published by Prentice-Hall Inc., 63-74, (1952).